Leggett-Garg inequality in electron interferometers

Clive Emary,[1] Neill Lambert,[2] and Franco Nori[2,3]
[1]*Institut für Theoretische Physik, Technische Universität Berlin, D-10623 Berlin, Germany*
[2]*Advanced Science Institute, The Institute of Physical and Chemical Research (RIKEN), Saitama 351-0198, Japan*
[3]*Physics Department, University of Michigan, Ann Arbor, Michigan 48109, USA*
(Received 9 October 2012; published 27 December 2012)

We consider the violation of the Leggett-Garg inequality in electronic Mach-Zehnder inteferometers. This setup has two distinct advantages over earlier quantum-transport proposals: Firstly, the required correlation functions can be obtained without time-resolved measurements. Secondly, the geometry of an interferometer allows one to construct the correlation functions from ideal negative measurements, which addresses the noninvasiveness requirement of the Leggett-Garg inequality. We discuss two concrete realizations of these ideas: the first in quantum Hall edge-channels, the second in a double quantum dot interferometer.

DOI: 10.1103/PhysRevB.86.235447 PACS number(s): 03.65.Ud, 73.23.−b, 03.65.Ta, 42.50.Lc

I. INTRODUCTION

Bell inequalities set bounds on the nature of the correlations between *multiple spatially*-separated entities within local hidden variable theories.[1,2] In contrast, Leggett-Garg inequalities (LGIs) set bounds on the *temporal* correlations of a *single* system,[3,4] and are derived under the assumptions of *macroscopic realism* (MR) and *noninvasive measurability* (NIM).[5]

Bell and Leggett-Garg inequalities are related in that their assumptions both imply the existence of a classical probability distribution that determines experimental outcomes. The probability amplitudes of quantum mechanics allow for violation of these inequalities: With Bell, the violation is due to entanglement between the systems; with Leggett-Garg, the violation occurs due to the superposition of system states and their collapse under measurement.

The simplest LGI, henceforth referred to as *the* LGI, reads

$$K \equiv C_{21} + C_{32} - C_{31} \leqslant 1, \tag{1}$$

where $C_{\alpha\beta} = \langle Q(t_\alpha)Q(t_\beta)\rangle$ is the correlation function of the dichotomous variable $Q = \pm 1$ at times t_α and t_β. Since the first experimental violation[6] of this inequality with weak measurements of a superconducting qubit, the Leggett-Garg inequality has been experimentally probed in systems as diverse as photons,[7–9] defect centers in diamond,[10] nuclear magnetic resonance,[11] and phosphorus impurities in silicon.[12] Whilst the subjects of these studies may not be macroscopic, the LGI performs a useful role for microscopic systems as an indicator that the device is operating beyond classical probability laws. Moreover, if one accepts that the alternative to classical probabilities is quantum mechanics, the LGI provides a decisive indicator of the "quantumness" of a system.[13]

In this paper, we are interested in the violation of the LGI in quantum transport, and in particular, in electron interferometers. Although there has been much work on Bell inequalities in electron transport, e.g., Refs. 14–23, the LGI has only relatively recently been considered in this setting.[24,25] Specifically, the charge flowing through a confined nanostructure, e.g., double quantum dot (DQD), has been shown to violate an inequality similar to Eq. (1) out of equilibrium.[24] Furthermore, the moment-generating function of charge transferred through a device has also been shown to be subject to a set of LG-style inequalities, which are violated for various quantum dot models. The violation of LGIs in excitonic transport has also attracted recent interest.[26,27]

There are several difficulties that make the investigation of the LGI in electronic transport challenging in practice. Ostensibly, the measurement of Eq. (1) requires time-resolved measurements where the time between successive measurements is smaller than the decoherence time of the system. For the double quantum dot of Ref. 24, for example, this decoherence time is of the order of 1 ns,[28] which makes the necessary time-resolved measurements very challenging (but, in principle, possible[29]). Furthermore, for the violation of Eq. (1) to be a meaningful indicator of nonclassical behavior, it must be ensured that the measurements are noninvasive. This "clumsiness loophole"[30] that allows violations of Eq. (1) to be associated with invasiveness of measurement, along with possible circumventions, has been the subject of much discussion.[3,27,31]

The transport setups we consider here are based on the electronic Mach-Zehnder Interferometer (MZI), and can overcome both of these problems.[32] The basic idea is that an electron traveling through a MZI can take one of two paths, and this path index defines the variable $Q = \pm 1$. Unidirectional passage of the electron through the system allows us to map the time indices of Eq. (1) onto positions within the interferometer. As we show below, this removes the need for time-resolved measurements.

We consider two realizations of the MZI in which measurements of Q are performed in two different ways. In the first, the MZI is formed from quantum Hall edge channels, a setup which has been realized experimentally[33–42] and also attracted a large degree of theoretical attention.[43–57] By interrupting the edge channels at various points and diverting electron flow to current meters, we show that K can be obtained from measurements of *mean currents* alone. Furthermore, due to the spatial separation of the $Q = +1$ and $Q = -1$ channels, our detectors interact with only one of the two Q states at any given time. Thus, our scheme provides a natural way to implement *ideal negative measurements*, as advanced by Leggett and Garg as a way to satisfy the NIM criterion.[3]

The second setup we consider is a MZI with a quantum dot (QD) in each arm. This geometry is similar to several experiments,[58–62] the difference here being that the dots are fed by two tunnel-coupled leads[63] rather than just one. The QDs are monitored by quantum point contacts, whose transmission is sensitive to the charge state of the QD.[64–69] In contrast with the first setup, electrons are not diverted out of the MZI at any point, and the influence of the detectors occurs as a pure dephasing effect. The three correlation function in Eq. (1) are obtained through a combination of mean currents, both through the MZI and the quantum point contacts, and zero-frequency noise measurements, which cross-correlate current fluctuations in the MZI and quantum point contacts. As in the previous scheme, we construct an ideal negative measurement scheme with this setup.

Both of these techniques exploit a combination of superpositions of paths through an interferometer combined with a gathering of "which-way" information to violate the LGI. The first setup is a particularly simple realization of the LGI, and is by no means restricted to transport, but could be used, e.g., with photons, atoms, or molecules.

The paper proceeds as follows. In Sec. II we describe the basics of testing the LGI in a MZI. Section III describes how this may be translated into experiments with quantum Hall effect edge channels. Finally, Sec. IV considers the alternative DQD-QPC geometry.

II. MACH-ZEHNDER INTERFEROMETER

We begin by describing an abstract version of our MZI scheme to outline the basic ideas. The MZI is a two-channel interferometer with two beamsplitters that divide the MZI into three zones which we label: 1, the input ports; 2, the arms of the interferometer; and 3, the output ports (see Fig. 1). We inject one electron at a time into the MZI, and the path taken by the electron will be the degree-of-freedom under test with $Q = +1$ when the electron is located in the upper channel of the MZI, and $Q = -1$ the lower. Since the electron passes sequentially through the three zones, we can map a measurement of Q at time t_α to a "which-way" measurement at any point in the region α of the interferometer. In particular, Q_1 and Q_3 are measured at the input and output ports, and Q_2 is measured by placing detectors in the arms of the interferometer at $2\pm$, where 2 refers to the zone, and $\pm$ the upper or lower channel. In this section we assume that we have ideal single-electron detectors that "click" on detecting an electron, which is then removed from the system (i.e., the detectors act essentially as electronic analogues of photodetectors). More realistic measurements in terms of currents are discussed in Sec. III.

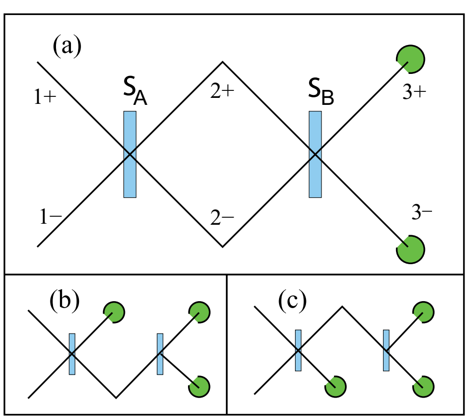

FIG. 1. (Color online) The Mach-Zehnder interferometer with three different detector configurations for the noninvasive measurement of the LGI of Eq. (1). Electrons are injected into the 1+ port. **(a)** Complete MZI configuration with detectors only at the final outputs $3\pm$. With this setup we can measure the probabilities $P^D_{3\pm}(1)$ and construct C_{31}. **(b)** An additional detector is inserted into the MZI + arm. With this configuration we can measure probabilities $P^D_{2+}(0)$ and $P^D_{3\pm;2+}(1,\cdot)$. **(c)** A detector in the − arm allows us to obtain $P^D_{2-}(0)$ and $P^D_{3\pm;2-}(1,\cdot)$. Combining the results of (b) and (c) allows us to construct correlation functions C_{21} and C_{32}.

A. Ideal negative measurements

A detector placed in one of the arms interacts strongly with electrons in that path (they are completely removed from the MZI) and has no effect on electrons in the other. With a detector placed at $Q = +1$, say, the absence of a detector response (combined with MR and ideal detectors) allows us to infer the state of the system ($Q = -1$) without any disruption. This is exactly the form of detector required to perform an ideal negative measurement as envisioned in Ref. 3.

To make the measurement scheme as simple as possible, let us inject electrons into the 1+ port, such that the initial state is known. [70] We do not need to measure in zone 1 and there is no question about the NIM of Q_1. The correlation function C_{21} and C_{31} boil down to measuring $\langle Q_2\rangle$ and $\langle Q_3\rangle$, respectively.

Let us define $P^D_{\alpha\pm}(n)$ as the probability that the detector placed at position $\alpha\pm$ either detects ($n = 1$) or fails to detect ($n = 0$) the electron. Since no further measurements are made past point 3, it is irrelevant whether we measure noninvasively or not at point 3. Placing detectors at $3\pm$, we measure the probabilities $P^D_{3\pm}(1)$, and the C_{31} correlation function can simplify be expressed as

$$C_{31} = P^D_{3+}(1) - P^D_{3-}(1). \tag{2}$$

The setup for this measurement is shown in Fig. 1(a).

Since, in measuring C_{21}, no further measurements are made after region 2, it is also not necessary to measure C_{21} noninvasively. We can measure $\langle Q_2\rangle$ (and thus C_{21}) by running the experiment once with a detector in channel 2+ , and once in 2− [Figs. 1(b) and 1(c)] and writing

$$C_{21} = P^D_{2+}(1) - P^D_{2-}(1). \tag{3}$$

It is perhaps instructive to discuss how to obtain this quantity using the ideal negative measurement technique and measure C_{21} in terms of the probabilities of absence of detector clicks. With the detector at 2+, we can equate the probability that no electron is detected, $P^D_{2+}(0)$, with the probability that the electron travels the path 2−. Swapping the detector to the other arm, we measure $P^D_{2-}(0)$ and infer the probability that the electron takes path 2+. Whence, we obtain the noninvasively measured

$$C_{21} = P^D_{2-}(0) - P^D_{2+}(0). \tag{4}$$

Since $P^D_{2\pm}(0) = 1 - P^D_{2\pm}(1)$, Eq. (3) and Eq. (4) give the same result.

We now consider C_{32}, where it is essential that we measure Q_2 noninvasively, since a subsequent measurement is performed. On the face of it, measuring C_{32} requires a correlation measurement between two detectors. This, however, is not the case, as we now show.

Let us begin by placing one detector at $2+$ and another one at $3+$ [Fig. 1(b)]. We can then obtain the four probabilities, $P^D_{3+,2+}(n,n')$, that the detectors at $3+$ and $2+$ give the results $n,n' = 0,1$, respectively. Of these, the one we are interested in is $P^D_{3+,2+}(1,0)$, since this allows us to infer (noninvasively) the probability that the electron took path $2-$ to detector $3+$. Moreover, we do not actually need to actively detect at $2+$, since, if the electron reaches the $3+$ detector, it is clear that it has not entered channel $2+$ (because the detector there would have removed the electron from the system).[71] With all four probabilities, $P^D_{3q,2q'}(1,\cdot)$, obtained in this noninvasive way, we can construct

$$C_{32} = -\sum_{q,q'=\pm} qq' P^D_{3q,2q'}(1,\cdot), \qquad (5)$$

where we have replaced the measurement value at position 2 with a dot to indicate that we do not actually have to measure there (the value is guaranteed to be zero).

In this way we obtain all the required correlation functions, measured noninvasively where necessary. Although we have concentrated on the simplest case here, the above noninvasive techniques are extensible to the case where the input state is unknown and all $C_{\alpha\beta}$ must be measured in a noninvasive way, or to more complicated LGIs.[11]

B. Leggett-Garg Inequality

The action of the MZI can be specified by two beamsplitter scattering matrices s_X; $X = A,B$. With $a_{\alpha q}$ the annihilation operator for an electron in channel αq, the beamsplitter input-output relations read

$$\begin{pmatrix} a_{2+} \\ a_{2-} \end{pmatrix} = s_A \begin{pmatrix} a_{1+} \\ a_{1-} \end{pmatrix}; \quad \begin{pmatrix} a_{3+} \\ a_{3-} \end{pmatrix} = s_B \begin{pmatrix} a_{2+} \\ a_{2-} \end{pmatrix}. \qquad (6)$$

Parameterizing the scattering matrices as

$$s_X = \begin{pmatrix} \cos(\frac{1}{2}\theta_X) & \sin(\frac{1}{2}\theta_X)e^{i\frac{1}{2}\phi_X} \\ -\sin(\frac{1}{2}\theta_X)e^{-i\frac{1}{2}\phi_X} & \cos(\frac{1}{2}\theta_X) \end{pmatrix}, \qquad (7)$$

we obtain the correlation functions

$$C_{21} = \cos\theta_A; \qquad (8)$$

$$C_{31} = \cos\theta_A \cos\theta_B - \sin\theta_A \sin\theta_B \cos\phi; \qquad (9)$$

$$C_{32} = \cos\theta_B, \qquad (10)$$

such that the LG correlator reads

$$K(\theta_A,\theta_B,\phi) = \cos\theta_A + \cos\theta_B - \cos\theta_A\cos\theta_B + \sin\theta_A\sin\theta_B\cos\phi, \qquad (11)$$

with $\phi = \frac{1}{2}(\phi_A - \phi_B)$ being the phase difference accumulated between the two paths. This is a familiar expression. If we identify $\theta_A = \Omega\tau_1$ and $\theta_B = \Omega\tau_2$, then Eq. (11) is exactly that obtained for a qubit evolving under the Hamiltonian $H = \frac{1}{2}\Omega\sigma_x$ measured in the σ_z basis at times t_1, $t_2 = t_1 + \tau_1$, and $t_3 = t_2 + \tau_2$. The properties of Eq. (11) are discussed in Sec. III.

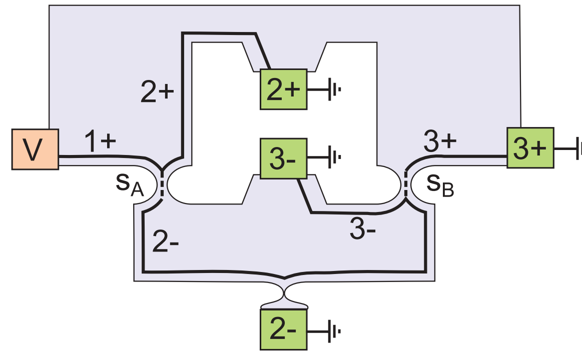

FIG. 2. (Color online) Quantum Hall edge-channel realization of the MZI setup for measurement of Leggett-Garg inequality. The MZI setup is similar to that of Ref. 33 but with two extra detectors (2±). These additional detectors can be isolated from the circuit by closing off the QPCs between them and the edge channel. The configuration shown has the detector at the 2+ position active such that transmission to beamsplitter B via channel 2+ is blocked, and the detector at 2− is pinched off. This detector combination corresponds to that of Fig. 1(b).

III. QUANTUM HALL EDGE-CHANNELS

Quantum Hall edge channels have been shown to allow a direct translation of the MZI into electronic transport experiments,[33–39,41] and Fig. 2 shows a sketch of the quantum Hall geometry needed to realize our proposal. Each channel in the MZI is realized with a single edge channel and the electronic beamsplitters are realized by quantum point contacts (QPCs). Backscattering is suppressed between edge channels such that transport is unidirectional. This setup is the same as the MZIs of experiment except for the addition of extra contacts to the arms of the interferometer. These contacts are connected to the edge channels via adjustable quantum point contacts, such that the detectors can be coupled into and out of the MZI as required. This method of coupling probes to the MZI arms has been realized in Ref. 41. Port $1+$ is raised to a voltage $+V$ and electrons are injected into this channel. The output ports (detectors) are all grounded. When the correlation function C_{31} is being measured, the detectors at $2\pm$ are not required and are isolated from the MZI by closing their QPCs (Fig. 2 shows detector $2-$ closed off in this way). To measure the remaining correlation functions, the detectors at $2\pm$ are, one then the other, connected into the MZI by opening up their respective QPCs. In Fig. 2, the detector at $2+$ is connected into the circuit and fully prevents electrons in channel $2+$ from reaching the outputs $3\pm$.

A. Current measurements

Let $\langle I_{\alpha q}\rangle$ be the mean stationary current flowing into output αq, given that when $\alpha = 3$, the detectors at positions $2\pm$ are closed off. Further, let $\langle I_{3q;2q'}\rangle$ be the current flowing at output $3q$ when the output at $2q'$ is open. Since, in the linear regime, the current operator for each output is $I_{\alpha q} = G_0 V a^\dagger_{\alpha q} a_{\alpha q}$, with $G_0 = e^2/h$ the conduction quantum,[72] these mean currents are proportional to the probability that an electron travels in the corresponding channel. The correlation functions required for the LGI can then be constructed, as with the CHSH inequality,[16,17,73] as

$$C_{\alpha 1} = \frac{\langle I_{\alpha+}\rangle - \langle I_{\alpha-}\rangle}{\langle I_{\alpha+}\rangle + \langle I_{\alpha-}\rangle}; \tag{12}$$

$$C_{32} = \frac{-\sum q q' \langle I_{3q;2q'}\rangle}{\sum \langle I_{3q;2q'}\rangle}. \tag{13}$$

Division by the sum of detector currents removes proportionality factors and, if all detectors are identical, also removes detector inefficiencies. Writing the scattering matrices as

$$s_X = \begin{pmatrix} r_X & t'_X \\ t_X & r'_X \end{pmatrix}, \tag{14}$$

we obtain the correlation functions

$$\begin{aligned} C_{21} &= |r_A|^2 - |t_A|^2; \\ C_{31} &= |r_B r_A + t'_B t_A|^2 - |t_B r_A + r'_B t_A|^2; \\ C_{32} &= |r_A|^2\{|r_B|^2 - |t_B|^2\} - |t_A|^2\{|t'_B|^2 - |r'_B|^2\}. \end{aligned} \tag{15}$$

With scattering matrices as in the previous section, the LG parameter K obtained from current measurements is the same as Eq. (11). This quantity is plotted in Fig. 3(a). A maximum violation of $K_{\max} = \frac{3}{2}$ is obtained for parameters $\theta_A = \theta_B = \pi/3$ and $\phi = 0$.

The violation of the LGI in this setup arises because the measurements at 2± remove electrons from the interferometer arms, preventing interference between the two paths. The presence of this interference in C_{31} combined with its absence in C_{32} leads to the violation.

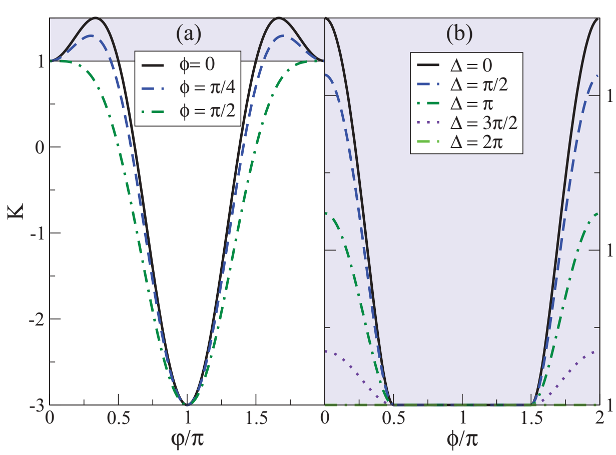

FIG. 3. (Color online) (a) LG correlator $K(\theta_A,\theta_B,\phi)$ of Eq. (11) as a function of the beamsplitter angle $\theta = \theta_A = \theta_B$ for three values of the phase $\phi = 0,\pi/4,\pi/2$. The shaded blue region indicated violation of the LG inequality ($K > 1$). The maximum violation, $K_{\max} = \frac{3}{2}$, occurs for $\phi = 0$ and, e.g., $\theta = \pi/3$. (b) The influence of dephasing. Shown is the LG correlator K of Eq. (16) maximized over $\theta_{A/B}$ as a function of the phase ϕ. Results shown for values of the dephasing parameter $\Delta/\pi = 0,\frac{1}{2},1,\frac{3}{2},2$. Violations of the LG are only observed for $\cos\phi > 0$.

B. Dephasing

Dephasing in edge-channel interferometers is a much-studied topic.[35–39,41,42,44–48,52–57] While it is clear that electron-electron interactions are ultimately responsible,[74] the details depend on the specifics of the particular realization. Here we take a very simple approach and phenomenologically account for the effects of dephasing by allowing the phase ϕ to fluctuate. We replace $\phi \to \phi + \delta\phi$ in Eq. (11) and integrate $\delta\phi$ over a flat distribution in the range $-\Delta/2 < \delta\phi < \Delta/2$. The resulting LG parameter with dephasing reads

$$\begin{aligned} K^{\mathrm{deph}} &= \cos\theta_A + \cos\theta_B - \cos\theta_A \cos\theta_B \\ &\quad + f(\Delta)\sin\theta_A \sin\theta_B \cos\phi. \end{aligned} \tag{16}$$

Here, $f(\Delta) = 2\Delta^{-1}\sin(\Delta/2)$ is the visibility of the AB oscillations, defined as

$$f = \frac{\langle I_{3+}(\phi=\pi)\rangle - \langle I_{3+}(\phi=0)\rangle}{\langle I_{3+}(\phi=\pi)\rangle + \langle I_{3+}(\phi=0)\rangle}, \tag{17}$$

evaluated with beamsplitter angles $\theta_A = \theta_B = \pi/2$. If all angles are freely variable, then the maximum value of the LGI function is

$$K^{\mathrm{deph}}_{\max}(\Delta) = \frac{1 + f(\Delta)\{1 + f(\Delta)\}}{1 + f(\Delta)}, \tag{18}$$

obtained for $\cos\theta_A = \cos\theta_B = [1 + f(\Delta)]^{-1}$. Within this dephasing model then, any nonzero visibility implies a violation of the LGI since the LG correlator $K^{\mathrm{deph}}_{\max}$ exceeds the classical value for all $f \neq 0$. For small visibilities, $f \ll 1$, we have $K^{\mathrm{deph}}_{\max}(\Delta) \approx 1 + f^2(\Delta)$. In the opposite limit, $(1-f) \ll 1$, we have $K^{\mathrm{deph}}_{\max}(\Delta) \approx \frac{3}{4}\{1 + f(\Delta)\}$.

One interesting feature occurs if we assume that the phase ϕ is fixed (e.g., we are not able to vary the magnetic field) and maximize over $\theta_{A/B}$ [see Fig. 3(b)]. Provided that $\cos\phi > 0$, the maximum value is

$$K^{\mathrm{deph}}_{\max(\theta_{A/B})}(\phi,\Delta) = f(\Delta)\cos\phi + \frac{1}{1 + f(\Delta)\cos\phi}, \tag{19}$$

found by setting $\cos\theta_A = \cos\theta_B = [1 + f(\Delta)\cos\phi]^{-1}$. If, however, $\cos\phi \leqslant 0$, the maximum value is just the classical value, $K^{\mathrm{deph}}_{\max(\theta_{A/B})} = 1$, found by setting $\cos\theta_A = \cos\theta_B = 1$. This reversion to the classical value occurs when the scalar product between the axis of the rotation of beamsplitter B and that of beamsplitter A becomes negative.

C. Multichannel case

The above scheme is easily modified to include multiple channels. We take the same geometry as before but assume that each lead supports M channels. The M channels of the upper lead are all associated with qubit state $Q = +1$; the M channels in the lower lead, with state $Q = -1$. The scattering matrices of Eq. (14) are thus generalized to $2M \times 2M$ matrices with $M \times M$ blocks, r_X, t_X, r'_X, and t'_X. Assuming a large source-drain voltage, such that all channels are equally populated, the correlation functions read:

$$C_{21} = \frac{1}{M}\mathrm{Tr}\{R_A - T_A\};$$

$$C_{32} = \frac{1}{M}\mathrm{Tr}\{R_A^\dagger(R_B - T_B) + T_A^\dagger(R'_B - T'_B)\};$$

$$C_{31} = \frac{1}{M}\mathrm{Tr}\{R_A^\dagger(R_B - T_B) - T_A^\dagger(R_B' - T_B')\} + \frac{1}{M}\mathrm{Tr}\{r_A t_A^\dagger(t_B'^\dagger r_B - r_B'^\dagger t_B) + t_A r_A^\dagger(r_B^\dagger t_B' - t_B^\dagger r_B')\}, \quad (20)$$

with $R_A = r_A^\dagger r_A$, $T_A = t_A^\dagger t_A$, etc. The second term in the expression for C_{31} arises from interference between the paths. In the single channel case, these results reduce to those of Eq. (15).

An important observation can be made about the multichannel case by considering the special case that the scattering matrices preserve the channel index, i.e., we essentially have M independent interferometers. In this case, the LG parameter reads $K = \frac{1}{M}\sum_{m=1}^{M} K^{(m)}$, where $K^{(m)}$ is the LG parameter for channel m. If we could tune by hand all the parameters of the scattering matrices, then the maximum violation of $K_{\max} = \frac{3}{2}$ can be reached. However, in an experiment, there will typically only be a few controllable parameters and this could make violations hard to observe. Let us assume that we can adjust the parameters such that one of the $K^{(m)}$ is maximized, $m = 1$, say. Whether we see a violation or not very much depends on what happens with the parameters of the other channels. If these parameters are all roughly similar to those of channel 1, then violations should still be observed. Generically, however, this will not be the case, and the $K^{(m)}$ for the other channels will take unrelated values in the range from -3 to $\frac{3}{2}$. The negative values are particulary troublesome as they will tend to overwhelm any positive contribution to the violation from other channels. This lack of controllability means that multichannel geometries are best avoided if violations of the LGI are sought.

IV. DOUBLE QUANTUM DOT INTERFEROMETER

The above MZI scheme functions by having the detectors remove electrons from the interferometer arms. In this section we study a second MZI realization which leaves the electrons within the system and the effects of measurement are only felt through dephasing. This second setup is shown in Fig. 4. As in the foregoing, the basic structure is of two (single-channel) leads that are joined at two beamsplitters. Beamsplitters

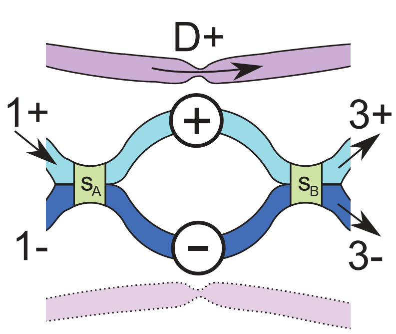

FIG. 4. (Color online) Sketch of a Mach-Zehnder interferometer with a quantum dot in each arm. The charge state of each QD can be monitored by the currents flowing through QPCs next to the dots. Here only the QPC monitoring the dot + is active, such that the correlation function to be measured is as in Fig. 1(b).

between non-edge-channel leads can be realized by tunnel junctions, as in the recent experiments by Yamamoto *et al.*[63] In each arm of the interferometer there is a QD and alongside each QD is a QPC charge detector. When connected to a voltage supply, the current flowing through the QPCs serves as a readout of the occupation of their respective QDs. Note that although similar detectors were used in, e.g., Refs. 75 and 76, the way in which they are used here is different.

A. Model

We first consider the system without detectors. Our MZI model is related to that of, e.g., Refs. 77 and 78, but with different leads. Far from the junctions, we describe the four leads as noninteracting Fermi reservoirs with Hamiltonian $H_{\rm res} = \sum \omega_{k\alpha q} c^\dagger_{k\alpha q} c_{k\alpha q}$ with k the wavenumber of the electron, and where $\alpha = 1{,}3$ and $q = \pm$ specify the lead (we set $\hbar = 1$ and ignore spin). We assume that there is but a single orbital of relevance in each dot and that the DQD system is in the strong Coulomb blockade regime, such that it is restricted to just three states: "empty," $|0\rangle$; or with one excess electron in either the upper or lower dots, $|+\rangle = d_+^\dagger|0\rangle$ and $|-\rangle = d_-^\dagger|0\rangle$, respectively. Assuming the dot levels are detuned by an energy ϵ from one another, the dot Hamiltonian reads $H_S = \frac{1}{2}\epsilon \sum_q q d_q^\dagger d_q$. In the following, we set $\epsilon = 0$ for simplicity.

We assume that the effect of the beamsplitters is to modify the amplitudes with which the leads couple to the QDs. So, for example, an electron in lead 1+ tunnels into a superposition of upper and lower dot states, with the details of the superposition being determined by the scattering matrix s_A. The tunnel Hamiltonian connecting lead and dots therefore reads

$$H_{\rm T} = \sum_k (\mathbf{C}^\dagger_{k1} \cdot s_A^\dagger \cdot \mathbf{d} + \mathbf{C}^\dagger_{k3} \cdot s_B \cdot \mathbf{d} + \text{H.c.}), \quad (21)$$

where $s_{A,B}$ are scattering matrices, assumed to be energy independent, $\mathbf{d} = (d_+, d_-)$ is a vector of dot operators, and $\mathbf{C}^\dagger_{k\alpha} = (T_{\alpha+} c^\dagger_{k\alpha+}, T_{\alpha-} c^\dagger_{k\alpha-})$ are vectors of lead operators with tunnel matrix elements $T_{\alpha s}$, also assumed to be energy independent. The corresponding sequential tunnel rates are $\Gamma_{\alpha q} = 2\pi |T_{\alpha q}|^2 \varrho_{\alpha q}$, where $\varrho_{\alpha q}$ is the density of states of reservoir αq, also assumed constant.

In the infinite-bias limit, the system can be described by a quantum master equation of Lindblad form.[79–81] Let us introduce the super-operator notations $\mathcal{J}[d]\rho = d\rho d^\dagger$ and $\mathcal{A}[d]\rho = -\frac{1}{2}\{d^\dagger d, \rho\}$,[82–84] and introduce the operators

$$\tilde{d}_{1q} = \sqrt{\Gamma_{1q}}\mathbf{e}_q \cdot s_A \cdot \mathbf{d}; \quad \tilde{d}_{3q} = \sqrt{\Gamma_{3q}}\mathbf{e}_q \cdot s_B \cdot \mathbf{d}, \quad (22)$$

with unit vectors $\mathbf{e}_+ = (1,0)$ and $\mathbf{e}_- = (0,1)$. With introduction of counting fields $\chi_{\alpha q}$ to facilitate the calculation of current statistics (see, e.g., Refs. 80 and 85), the χ-resolved master equation for the DQD system reads

$$\dot{\rho}(\chi) = -i[H_S, \rho] + \sum_{\alpha q}(e^{i\chi_{\alpha q}}\mathcal{J}[\tilde{d}_{\alpha q}] - \mathcal{A}[\tilde{d}_{\alpha q}])\rho. \quad (23)$$

The QDs are monitored by QPCs in a setup similar to the single dot in an interferometer in the experiment of Ref. 65. In including the detectors in our theory, we follow Gurvitz.[64,67]

When dot q is unoccupied, the Hamiltonian for QPC Dq reads

$$H_{Dq} = \sum_{ks} \omega^D_{ksq} a^\dagger_{ksq} a_{ksq} + \Omega_q \sum_k a^\dagger_{kLq} a_{kRq} + \text{H.c}, \quad (24)$$

where ω^D_{ksq} is the energy of an electron in state k on side $s = L,R$ of the the QPC, and Ω_q is the coupling amplitude between the two sides (assumed energy independent). When dot q is occupied, we assume that this Hamiltonian is modified such that the coupling constants shift to different values, $\Omega_q \to \Omega'_q$. In the limit of large bias across the QPC, the detector at location q gives rise to an extra Liouvillian

$$\mathcal{W}_{Dq}(\chi_{Dq}) = e^{i\chi_{Dq}} \mathcal{J}[\tilde{d}_{Dq}] - \mathcal{A}[\tilde{d}_{Dq}], \quad (25)$$

which adds to the DQD Liouvillian. Here, $\tilde{d}_{Dq} = \sqrt{\gamma'_q}|q\rangle\langle q| + \sqrt{\gamma_q}(1 - |q\rangle\langle q|)$ with γ_q the rate of electron transfer through the QPC q when its dot is empty, and γ'_q the rate when the dot is occupied. The counting field χ_{Dq} here allows us to calculate the statistics of the detector currents. Microscopically, the rates are $\gamma_q = 2\pi|\Omega_q|^2 \rho_{Lq}\rho_{Rq} V_{Dq}$ and $\gamma'_q = 2\pi|\Omega'_q|^2 \rho_{Lq}\rho_{Rq} V_{Dq}$, with ρ_{sq} the density of states of the QPC reservoir sq and V_{Dq} the applied voltage. Detectors may be decoupled or coupled from the MZI-QD system by adjusting the QPC voltages such that the differences between the amplitudes Ω_q and Ω'_q is either zero (decoupled) or finite (coupled). Here, we only couple at most one detector to the system at a given time. Furthermore, we assume balanced detectors such that with the $D+$ detector coupled we have $\gamma_+ = \gamma$, $\gamma'_+ = \gamma'$, and $\gamma_- = \gamma'_- = 0$, and when the $D-$ detector is coupled we have $\gamma_- = \gamma$, $\gamma'_- = \gamma'$, and $\gamma_+ = \gamma'_+ = 0$,

B. Current, correlation functions and probabilities

Our approach to measuring the LGI with this setup is similar to that with the quantum Hall edge channels with the main exception being how C_{32} is obtained. We inject electrons into the + channel of lead 1 and close the 1− channel: $\Gamma_{1+} \to \Gamma_L$ and $\Gamma_{1-} \to 0$. For simplicity, we set the output rates equal: $\Gamma_{3+} = \Gamma_{3-} = \Gamma_R$.

To obtain C_{31}, we switch off the QPC detectors and measure the output currents at 3±. Arranging the elements of the density matrix into a vector in the basis (00, ++, −−, +−, −+), the stationary state of the DQD system reads

$$\rho_{\text{stat}} = \frac{1}{2\Gamma}(2\Gamma_R, \Gamma_L(1+\cos\theta_A), \Gamma_L(1-\cos\theta_A), - e^{i\phi_A/2}\Gamma_L \sin\theta_A, - e^{-i\phi_A/2}\Gamma_L \sin\theta_A), \quad (26)$$

with total width $\Gamma = \Gamma_L + \Gamma_R$. Here, we have assumed the same scattering matrices as in Eq. (7). The total current flowing is $\langle I\rangle_{\text{tot}} = \langle I\rangle_{1+} = \Gamma_L\Gamma_R/\Gamma$, which is divided between the output ports as

$$\langle I\rangle_{3\pm} = \frac{\langle I\rangle_{\text{tot}}}{2}(1 \pm \cos\theta_A\cos\theta_B \mp \cos\phi\sin\theta_A\sin\theta_B).$$

Constructing C_{31} as in Eq. (12) we obtain

$$C_{31} = \cos\theta_A\cos\theta_B - \cos\phi\sin\theta_A\sin\theta_B, \quad (27)$$

which agrees with that of Eq. (9).

Next we can obtain C_{21} by turning on the QPC detectors one at a time. As shown in Ref. 64, the mean current flowing through the QPC can be used to extract the mean current flowing through the corresponding dot. With a detector coupled to dot q, the current through the detector is

$$\langle I_{Dq}\rangle = \frac{\langle I\rangle_{\text{tot}}}{2\Gamma_R}\left[\gamma\left(1 + 2\frac{\Gamma_R}{\Gamma_L}\right) + \gamma' + q(\gamma' - \gamma)\cos\theta_A\right].$$

The current flowing through the QPC when the DQD is empty is $\langle I^0_{Dq}\rangle = \gamma$, such that the difference is

$$\langle \Delta I_{Dq}\rangle = \langle I_{Dq}\rangle - \langle I^0_{Dq}\rangle = \frac{\gamma'_q - \gamma_q}{2\Gamma_R}\langle I\rangle_{\text{tot}}(1 + q\cos\theta_A), \quad (28)$$

which is proportional to the probability that an electron takes the path $2q$. Assuming balanced detectors, we obtain

$$C_{21} = \frac{\langle\Delta I_{D+}\rangle - \langle\Delta I_{D-}\rangle}{\langle\Delta I_{D+}\rangle + \langle\Delta I_{D-}\rangle} = \cos\theta_A, \quad (29)$$

as in Eq. (12).

Whereas these two correlation functions can be determined with just mean-current measurements, to determine C_{32} we need to consider current cross correlations. Let us first imagine that we can measure the current through dot q. Then, in the limit $\Gamma_L \to 0$, such that there is only ever at most one electron in the interferometer at a given time, the zero-frequency noise correlator

$$S_{3q'2q} \equiv \tfrac{1}{2}\int dt \langle\{I_{3q'}, I_{2q}\}\rangle_c, \quad (30)$$

where $\langle\ldots\rangle_c$ denotes the cumulant average, is proportional to the joint probability, $P_{3q'2q}$, that the electron travels through dot q and ends up at output $3q'$. This result follows in the same way as in Ref. 16, the difference here being that we correlate the position of a single electron in subsequent regions, as opposed to the correlation of two spatially-separate electrons. Measuring all four such correlators, we obtain the probabilities

$$P_{3q'2q} = \frac{S_{3q'2q}}{\sum_{r'r} S_{3r'2r}}. \quad (31)$$

From these directly-obtained probabilities, we construct the ideal-negative-measurement ones as

$$P^{\text{INM}}_{3q'2q} = P_{3q'} - P_{3q'2\overline{q}}, \quad (32)$$

where $\overline{q} = -q$ and the total probability at output $3q'$ is obtained from the currents

$$P_{3q} = \frac{\langle I_{3q}\rangle}{\sum_r \langle I_{3r}\rangle}. \quad (33)$$

These relations follow from charge conservation and the unidirectional nature of the transport.

The QPC detectors couple not to the current flowing through the dots, but rather to their occupations. In terms of the zero-frequency correlation function between current fluctuations in the QPC and those in one of the 3± ports,

$$S_{3q'Dq} \equiv \frac{1}{2}\int dt \langle\{I_{3q'}, I_{Dq}\}\rangle_c, \quad (34)$$

the required probabilities read

$$P_{3q'2q} = \frac{\langle\Delta I_{Dq}\rangle S_{3q'Dq}}{\sum_{r'r}\langle\Delta I_{Dr}\rangle S_{3r'Dr}}. \quad (35)$$

This can be understood as follows. Whereas $S_{3q'2q}$ correlates two delta-function peaks corresponding to the passage of the electron through the regions 2 and 3, $S_{3q'Dq}$ correlates a delta function in region 3 with a signal of finite duration in region 2, which corresponds to the finite time for which the dot is occupied. This mean occupation time is proportional to the inverse of mean current through the dot, which can be obtained (up to a proportionality constant) from the mean detector current $\langle \Delta I_{Dq} \rangle$.

Calculating these probabilities, we find that in the limit $\Gamma_L \to 0$, the third correlation function reads

$$C_{32} = \cos\theta_B, \quad (36)$$

in accordance with Eq. (10). Since, in the $\Gamma_L \to 0$ limit, all three correlation functions are identical with their ideal counterparts, the LGI for this setup is identical to that of Eq. (11). In the way that we have described the QPC detectors here, it does not make any difference whether we calculate K using the ideal negative measurement probabilities or the direct ones since, in our theoretical description, the QPC detectors act as ideal detectors and only influence the system through their dephasing effect. Experimentally, the ideal negative measurement protocol should be used, and actually, the comparison between the case with ideal negative measurement and that without would give an interesting method for studying to what extent the QPC measurements are noninvasive. Let us just add that, whilst the above results were derived in the symmetric case with $\Gamma_{R+}/\Gamma_{R-} = 1$ and with balanced detector rates, if these ratios are unequal but known, then the difference can be accounted for by weighting the terms in the correlation functions accordingly.

C. Dephasing

A simple way to include the effects of dephasing in this model is to "leave the detectors switched on" when calculating C_{31}. With empty and occupied rates γ_{dephase} and γ'_{dephase}, the measured K function has the form of Eq. (16), with the function $f(\Delta)$ replaced by

$$f = \left[1 + \frac{\{(\gamma'_{\text{dephase}})^{1/2} - (\gamma_{\text{dephase}})^{1/2}\}^2}{2\Gamma_R}\right]^{-1}. \quad (37)$$

The ideal no-dephasing case has $f = 1$, whereas $f = 0$ gives the classical limit. To obtain strong violations of the LGI therefore requires that the difference in rates γ'_{dephase} and γ_{dephase} is small compared with the tunnel rate Γ_R.

D. Detection errors

Just as the direct relation between the Bell inequalities and noise measurements of, e.g., Refs. 16 and 17 relies on the weak-tunnel limit,[18–21] so it is here that our measurements are only isomorphic with those required by the LGI in the $\Gamma_L \to 0$ limit. Away from this limit, there exists the possibility that our measurements mistakenly correlate subsequent electrons, rather than the same electron with itself.

The LGI quantity can be calculated using the currents and zero-frequency noise, as described above, away from the $\Gamma_L \to 0$ limit to assess the error. Assuming for simplicity that the detector is faster than the system dynamics $\gamma' - \gamma \gg \Gamma_{L/R}$ (although the general case can easily be investigated too), we obtain for the LG correlator

$$K' = \frac{1}{(\Gamma_L - \Gamma_R)\Gamma_R}\{[-(\Gamma_L + \Gamma_R)^2 + \Gamma_L(\Gamma_L + 3\Gamma_R)\cos^2\theta_A] \times \cos\theta_B + (\Gamma_L - \Gamma_R)\Gamma_R[2\cos\theta_A \sin^2(\theta_B/2) + \cos\phi \sin\theta_A \sin\theta_B]\}. \quad (38)$$

This expression is again maximized with $\cos\phi = 1$, but, unlike the $\Gamma_L \to 0$ case, the maximizing angles θ_A and θ_B are not equal. If we assume that $\Gamma_L/\Gamma_R \ll 1$, we can expand to leading order ($\gamma' - \gamma \to \infty$) to obtain

$$K' = K + 3\frac{\Gamma_L}{\Gamma_R}\cos\theta_B \sin^2\theta_A + O\left(\left(\frac{\Gamma_L}{\Gamma_R}\right)^2\right),$$

where K is the $\Gamma_L \to 0$ value. We can also calculate the corresponding quantity in the classical limit [this we do by calculating C_{31} in limit $(\gamma'_{\text{dephase}} - \gamma_{\text{dephase}}) \to \infty$]. In this case, we obtain $C_{31}^{\text{cl}} = \cos\theta_A \cos\theta_B$, and the expansion of $B' = C_{21} + C_{32} - C_{31}^{\text{cl}}$ for small Γ_L gives

$$B' = B + 3\frac{\Gamma_L}{\Gamma_R}\cos\theta_B \sin^2\theta_A + O\left(\left(\frac{\Gamma_L}{\Gamma_R}\right)^2\right), \quad (39)$$

where $B = \cos\theta_A + \cos\theta_B - \cos\theta_A\cos\theta_B$ is the classical value in the ideal case which, when maximized gives $B_{\text{max}} = 1$, the bound of Eq. (1). Maximizing B' over the angles, we obtain a value bigger than unity. To lowest order then, classical and quantum LG correlators are affected in the same way. Figure 5 shows the maximum values of both quantum and classical correlators.

Thus, assuming that we know the ratio of Γ_L/Γ_R from current and noise measurements, the effects of a finite tunneling rate Γ_L can be included in the assessment of whether LGI is violated or not. The conservative approach is to say that the quantity $(K'_{\text{max}} - \frac{3}{2})$ represents a systematic error in the measurement, and assuming that this error works against us, we can only conclude that we violate the LGI when the measured value of K exceeds unity by an amount equal to this

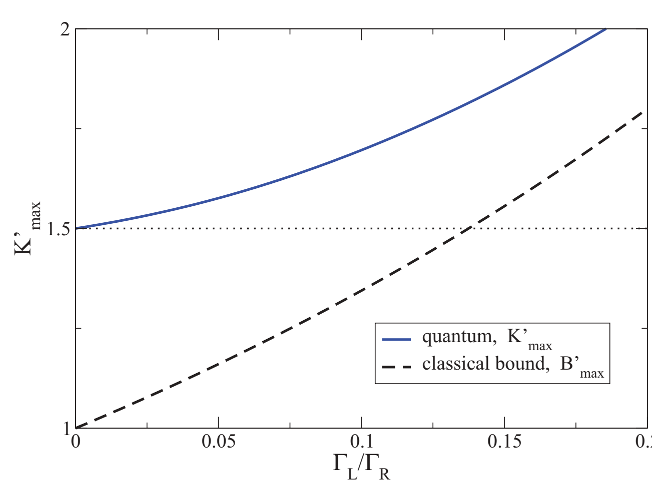

FIG. 5. (Color online) The maximum value K'_{max} (blue solid line) and the corresponding classical value B'_{max} (black dashed line) away from the $\Gamma_L \to 0$ limit. Both are higher than their ideal $\Gamma_L \to 0$ values. A symmetric system was assumed and the fast detector limit $(\gamma' - \gamma)/\Gamma_R \to \infty$ taken.

error. Alternatively, one can say that since one knows how the classical bound behaves at finite Γ/Γ_R, we can simply use $B'_{\rm max}$ of Eq. (39) as a bound. However, provided that we are in the correct operating limit of $\Gamma_L/\Gamma_R \ll 1$, these modifications will be very small, such that whether they are taken into account or not will only effect the question of violation in marginal cases.

V. CONCLUSIONS

We have considered the violation of the LGI in MZ inteferometer geometries. The key to the violation is a combination of the interference at the second beamsplitter and the inhibition of this interference by the measurement process. In the two proposals we have considered this inhibition occurs in two different ways. In the first realization, we physically interrupt transmission through one of the arms of the MZI, obviously preventing interference. On the other hand, in the DQD proposal, the detectors act in a more traditional way and introduce dephasing between the paths. The difference between these two approaches gives rise to two different detection schemes. In the first, the LGI correlation functions can be obtained with current measurements alone. In the second, because electrons are not removed from the system, we need the information about which path they have taken through the interferometer. As we have shown, zero-frequency noise measurements suffice for this.

In this MZ geometry both the state of the electron and measurement time are mapped onto real-space coordinates—the qubit states $Q = \pm$ are physically separate paths, and the regions within the interferometer correspond to different time instances. This mapping has several advantages for seeking a violation of the LGI in transport. The mapping of the time coordinate means that we do not need to make time-resolved correlation measurements. Furthermore, the spatial separation of the qubit degrees of freedom facilitates the realization of ideal negative measurement, since it is relatively easy to couple to just one of the qubit states when they are spatially distinct. In this respect, increasing the separation of the detector arms should decrease the plausibility of claims that detection in one arm is, from a macro-realist point of view, influencing the other.

The general principles described here can easily be extended to further systems. Within transport, for example, our second scheme could also be realized with an edge-channel MZI plus QPC detector channel without the quantum dots.[40,51–53] An alternative setting for the realization of our first scheme might be the flying qubit experiment of Ref. 63, which is essentially a MZI away from the quantum Hall regime. Two challenges are obvious with this realization. Firstly, the leads reported in the experiment have multiple channels, which potentially gives rise to the problems discussed in Sec. III C. The second problem is that of backscattering at the beamsplitters and detectors, which has (justifiably) been neglected here but probably can not be eliminated in setups such as that of Ref. 63. A further interesting prospect is the realization of the MZI in single-electron quantum optics.[86–88]

Applications away from electronic transport are also possible. The application of the first scheme in optics is obvious. Indeed, a classical wave, once interpreted in terms of individual photons, could be able to violate Eq. (1). Going further, the same principles could be used to test the LGI with electrons in free space, neutrons, atoms, and molecules, all of which have had interference experiments in the MZI geometry conducted on them.[89,90] Of these, molecules offer the most exciting prospect, as there the nature of the coherence being tested could potentially be macroscopic, in line with the original goals of Ref. 3.

ACKNOWLEDGMENTS

We are grateful to S. Huelga, Y. Ota, P. Roche, P. Samuelsson, and M. Yamamoto for useful discussions. This work was supported by the DFG through SFB 910. F.N. acknowledges partial support from the ARO, JSPS-RFBR Contract No. 12-02-92100, MEXT Kakenhi on Quantum Cybernetics, and the JSPS-FIRST Program.

[1] J. S. Bell, Physics **1**, 195 (1964).
[2] J. S. Bell, *Speakable and Unspeakable in Quantum Mechanics*, 2nd ed. (Cambridge University Press, Cambridge, 2004).
[3] A. J. Leggett and A. Garg, Phys. Rev. Lett. **54**, 857 (1985).
[4] A. J. Leggett, J. Phys.: Condens. Matter **14**, R415 (2002).
[5] From Ref. 3, these assumptions are as follows. "*Macroscopic realism:* A macroscopic system with two or more macroscopically distinct states available to it will, at all times, be in one or the other of these states. *Noninvasive measurability*: It is possible, in principle, to determine the state of the system with arbitrary small perturbation on its subsequent dynamics." To clarify further, a noninvasive measurement in this context is one that, under a macroscopic real understanding of the system, would leave the state of the system unchanged by the measurement. This clarification is important because a measurement on a quantum system can be "noninvasive" in the sense that it would not disturb a macroscopic real system, and yet still be invasive in actuality because it causes a collapse of the systems wave function (a concept absent from a macroscopic real description). More information can be found in Refs. 3 and 4.
[6] A. Palacios-Laloy, F. Mallet, F. Nguyen, P. Bertet, D. Vion, D. Esteve, and A. N. Korotkov, Nat. Phys. **6**, 442 (2010).
[7] M. E. Goggin, M. P. Almeida, M. Barbieri, B. P. Lanyon, J. L. O'Brien, A. G. White, and G. J. Pryde, Proc. Natl. Acad. Sci. USA **108**, 1256 (2011).
[8] J.-S. Xu, C.-F. Li, X.-B. Zou, and G.-C. Guo, Sci. Rep. **1**, 101 (2011).
[9] J. Dressel, C. J. Broadbent, J. C. Howell, and A. N. Jordan, Phys. Rev. Lett. **106**, 040402 (2011).
[10] G. Waldherr, P. Neumann, S. F. Huelga, F. Jelezko, and J. Wrachtrup, Phys. Rev. Lett. **107**, 090401 (2011).
[11] V. Athalye, S. S. Roy, and T. S. Mahesh, Phys. Rev. Lett. **107**, 130402 (2011).

[12]G. C. Knee, S. Simmons, E. M. Gauger, J. J. Morton, H. Riemann, N. V. Abrosimov, P. Becker, H.-J. Pohl, K. M. Itoh, M. L. Thewalt, G. A. D. Briggs, and S. C. Benjamin, Nat. Commun. **3**, 606 (2012).
[13]A. Miranowicz, M. Bartkowiak, X. Wang, Y.-x. Liu, and F. Nori, Phys. Rev. A **82**, 013824 (2010).
[14]S. Kawabata, J. Phys. Soc. Jpn. **70**, 1210 (2001).
[15]N. M. Chtchelkatchev, G. Blatter, G. B. Lesovik, and T. Martin, Phys. Rev. B **66**, 161320 (2002).
[16]P. Samuelsson, E. V. Sukhorukov, and M. Büttiker, Phys. Rev. Lett. **91**, 157002 (2003).
[17]C. W. J. Beenakker, C. Emary, M. Kindermann, and J. L. van Velsen, Phys. Rev. Lett. **91**, 147901 (2003).
[18]P. Samuelsson, E. V. Sukhorukov, and M. Büttiker, Phys. Rev. Lett. **92**, 026805 (2004).
[19]A. V. Lebedev, G. B. Lesovik, and G. Blatter, Phys. Rev. B **71**, 045306 (2005).
[20]C. Beenakker, in *Quantum Computers, Algorithms and Chaos*, Proc. Int. School Phys. E. Fermi, Vol. 162, edited by G. Casati (IOS Press, Amsterdam, 2006).
[21]P. Samuelsson, I. Neder, and M. Büttiker, Phys. Rev. Lett. **102**, 106804 (2009).
[22]C. Emary, Phys. Rev. B **80**, 161309 (2009).
[23]A. Bednorz and W. Belzig, Phys. Rev. B **83**, 125304 (2011).
[24]N. Lambert, C. Emary, Y.-N. Chen, and F. Nori, Phys. Rev. Lett. **105**, 176801 (2010).
[25]C. Emary, Phys. Rev. B **86**, 085418 (2012).
[26]Y.-N. Sun, Y. Zou, R.-C. Ge, J.-S. Tang, and C.-F. Li, Chinese Phys. Lett. **29**, 120302 (2012).
[27]M. M. Wilde, J. M. McCracken, and A. Mizel, Proc. R. Soc. A **466**, 1347 (2010).
[28]T. Hayashi, T. Fujisawa, H. D. Cheong, Y. H. Jeong, and Y. Hirayama, Phys. Rev. Lett. **91**, 226804 (2003).
[29]K. D. Petersson, J. R. Petta, H. Lu, and A. C. Gossard, Phys. Rev. Lett. **105**, 246804 (2010).
[30]M. Wilde and A. Mizel, Found. Phys. **42**, 256 (2012).
[31]L. E. Ballentine, Phys. Rev. Lett. **59**, 1493 (1987); A. J. Leggett and A. Garg, *ibid.* **59**, 1621 (1987); A. Peres, *ibid.* **61**, 2019 (1988); A. J. Leggett and A. Garg, *ibid.* **63**, 2159 (1989); C. D. Tesche, *ibid.* **64**, 2358 (1990); A. Elby and S. Foster, Phys. Lett. A **166**, 17 (1992); J. P. Paz and G. Mahler, Phys. Rev. Lett. **71**, 3235 (1993); F. Benatti, G. Ghirardi, and R. Geassi, Il Nuovo Cimento B (1971-1996) **110**, 593 (1995); T. Calarco and R. Onofrio, Phys. Lett. A **198**, 279 (1995); R. Onofrio and T. Calarco, *ibid.* **208**, 40 (1995).
[32]After the preparation of this manuscript we learned that violations of the LGI in the MZI were also considered in the preprint J. Kofler and C. Brukner, arXiv:1207.3666.
[33]Y. Ji, Y. Chung, D. Sprinzak, M. Heiblum, D. Mahalu, and H. Shtrikman, Nature (London) **422**, 415 (2003).
[34]I. Neder, M. Heiblum, Y. Levinson, D. Mahalu, and V. Umansky, Phys. Rev. Lett. **96**, 016804 (2006).
[35]L. V. Litvin, H.-P. Tranitz, W. Wegscheider, and C. Strunk, Phys. Rev. B **75**, 033315 (2007).
[36]P. Roulleau, F. Portier, D. C. Glattli, P. Roche, A. Cavanna, G. Faini, U. Gennser, and D. Mailly, Phys. Rev. B **76**, 161309 (2007).
[37]I. Neder and E. Ginossar, Phys. Rev. Lett. **100**, 196806 (2008).
[38]P. Roulleau, F. Portier, P. Roche, A. Cavanna, G. Faini, U. Gennser, and D. Mailly, Phys. Rev. Lett. **100**, 126802 (2008).
[39]P. Roulleau, F. Portier, P. Roche, A. Cavanna, G. Faini, U. Gennser, and D. Mailly, Phys. Rev. Lett. **101**, 186803 (2008).
[40]D.-I. Chang, G. L. Khym, K. Kang, Y. Chung, H.-J. Lee, M. Seo, M. Heiblum, D. Mahalu, and V. Umansky, Nat. Phys. **4**, 205 (2008).
[41]P. Roulleau, F. Portier, P. Roche, A. Cavanna, G. Faini, U. Gennser, and D. Mailly, Phys. Rev. Lett. **102**, 236802 (2009).
[42]A. Helzel, L. V. Litvin, I. P. Levkivskyi, E. V. Sukhorukov, W. Wegscheider, and C. Strunk, arXiv:1211.5951.
[43]G. Seelig and M. Büttiker, Phys. Rev. B **64**, 245313 (2001).
[44]F. Marquardt and C. Bruder, Phys. Rev. Lett. **92**, 056805 (2004).
[45]F. Marquardt and C. Bruder, Phys. Rev. B **70**, 125305 (2004).
[46]H. Förster, S. Pilgram, and M. Büttiker, Phys. Rev. B **72**, 075301 (2005).
[47]V. S.-W. Chung, P. Samuelsson, and M. Büttiker, Phys. Rev. B **72**, 125320 (2005).
[48]E. V. Sukhorukov and V. V. Cheianov, Phys. Rev. Lett. **99**, 156801 (2007).
[49]H. Förster, P. Samuelsson, and M. Büttiker, New J. Phys. **9**, 117 (2007).
[50]H. Förster, P. Samuelsson, S. Pilgram, and M. Büttiker, Phys. Rev. B **75**, 035340 (2007).
[51]I. Neder, M. Heiblum, D. Mahalu, and V. Umansky, Phys. Rev. Lett. **98**, 036803 (2007).
[52]I. Neder, F. Marquardt, M. Heiblum, D. Mahalu, and V. Umansky, Nat. Phys. **3**, 534 (2007).
[53]I. Neder and F. Marquardt, New J. Phys. **9**, 112 (2007).
[54]S.-C. Youn, H.-W. Lee, and H.-S. Sim, Phys. Rev. Lett. **100**, 196807 (2008).
[55]I. P. Levkivskyi and E. V. Sukhorukov, Phys. Rev. B **78**, 045322 (2008).
[56]I. P. Levkivskyi and E. V. Sukhorukov, Phys. Rev. Lett. **103**, 036801 (2009).
[57]P. Degiovanni, C. Grenier, and G. Fève, Phys. Rev. B **80**, 241307 (2009).
[58]A. W. Holleitner, C. R. Decker, H. Qin, K. Eberl, and R. H. Blick, Phys. Rev. Lett. **87**, 256802 (2001).
[59]M. Sigrist, A. Fuhrer, T. Ihn, K. Ensslin, S. E. Ulloa, W. Wegscheider, and M. Bichler, Phys. Rev. Lett. **93**, 066802 (2004).
[60]T. Ihn, M. Sigrist, K. Ensslin, W. Wegscheider, and M. Reinwald, New J. Phys. **9**, 111 (2007).
[61]A. Muhle, W. Wegscheider, and R. J. Haug, Appl. Phys. Lett. **92**, 013126 (2008).
[62]T. Hatano, T. Kubo, Y. Tokura, S. Amaha, S. Teraoka, and S. Tarucha, Phys. Rev. Lett. **106**, 076801 (2011).
[63]M. Yamamoto, S. Takada, C. Bauerle, K. Watanabe, A. D. Wieck, and S. Tarucha, Nat. Nanotechnol. **7**, 247 (2012).
[64]S. A. Gurvitz, Phys. Rev. B **56**, 15215 (1997).
[65]E. Buks, R. Schuster, M. Heiblum, D. Mahalu, and V. Umansky, Nature (London) **391**, 871 (1998).
[66]A. N. Korotkov, Phys. Rev. B **60**, 5737 (1999).
[67]S. Gurvitz, Phys. Lett. A **311**, 292 (2003).
[68]D. V. Averin and E. V. Sukhorukov, Phys. Rev. Lett. **95**, 126803 (2005).
[69]S. Ashhab, J. Q. You, and F. Nori, New J. Phys. **11**, 083017 (2009).
[70]It is known that the initial state of the system does not affect the degree of violation of the LGI (Ref. 91).
[71]We do not actually need it to be a detector at $2\pm$, anything that removes the electron from the system would suffice. However, seeing as we need detectors for measuring C_{21}, it seems sensible to use these.

[72] Y. M. Blanter and M. Büttiker, Phys. Rep. **336**, 1 (2000).
[73] J. F. Clauser, M. A. Horne, A. Shimony, and R. A. Holt, Phys. Rev. Lett. **23**, 880 (1969).
[74] A. Yacoby, U. Sivan, C. P. Umbach, and J. M. Hong, Phys. Rev. Lett. **66**, 1938 (1991).
[75] R. Ruskov, A. N. Korotkov, and A. Mizel, Phys. Rev. Lett. **96**, 200404 (2006).
[76] A. N. Jordan, A. N. Korotkov, and M. Büttiker, Phys. Rev. Lett. **97**, 026805 (2006).
[77] F. Marquardt and C. Bruder, Phys. Rev. B **68**, 195305 (2003).
[78] D. Urban and J. König, Phys. Rev. B **79**, 165319 (2009).
[79] S. A. Gurvitz, Phys. Rev. B **57**, 6602 (1998).
[80] D. A. Bagrets and Y. V. Nazarov, Phys. Rev. B **67**, 085316 (2003).
[81] T. Brandes, Phys. Rep. **408**, 315 (2005).
[82] C. W. Gardiner, Phys. Rev. Lett. **70**, 2269 (1993).
[83] H. J. Carmichael, Phys. Rev. Lett. **70**, 2273 (1993).
[84] H. M. Wiseman, Phys. Rev. A **49**, 2133 (1994).
[85] L. S. Levitov, H. Lee, and G. B. Lesovik, Journal Mathematical Physics **37**, 4845 (1996); L. S. Levitov, in *Quantum Noise in Mesoscopic Physics*, Nato Science series, Vol. 97, edited by Y. V. Nazarov (Kluwer, Dordrecht, 2002), p. 373.
[86] G. Fève, A. Mahé, J.-M. Berroir, T. Kontos, B. Plaçais, D. C. Glattli, A. Cavanna, B. Etienne, and Y. Jin, Science **316**, 1169 (2007).
[87] G. Haack, M. Moskalets, J. Splettstoesser, and M. Büttiker, Phys. Rev. B **84**, 081303 (2011).
[88] E. Bocquillon, F. D. Parmentier, C. Grenier, J.-M. Berroir, P. Degiovanni, D. C. Glattli, B. Plaçais, A. Cavanna, Y. Jin, and G. Fève, Phys. Rev. Lett. **108**, 196803 (2012).
[89] J. Schmiedmayer, M. S. Chapman, C. R. Ekstrom, T. D. Hammond, D. A. Kokorowski, A. Lenef, R. A. Rubenstein, E. T. Smith, and D. E. Pritchard, in *Atom Interferometry*, edited by P. R. Berman (Academic Press, San Diego, 1997), pp. 1–83.
[90] A. D. Cronin, J. Schmiedmayer, and D. E. Pritchard, Rev. Mod. Phys. **81**, 1051 (2009).
[91] G. C. Knee, E. M. Gauger, G. A. D. Briggs, and S. C. Benjamin, New J. Phys. **14**, 058001 (2012).